A column generation approach for evaluating delivery efficiencies of collimator technologies in IMRT treatment planning

M Gören and Z C Taşkın

Department of Industrial Engineering, Boğaziçi University, 34342, Bebek, Istanbul, Turkey

E-mail: merve.goren@boun.edu.tr, caner.taskin@boun.edu.tr

Abstract. Collimator systems used in Intensity Modulated Radiation Therapy (IMRT) can form different geometric aperture shapes depending on their physical capabilities. We compare the efficiency of using regular, rotating and dual multileaf collimator (MLC) systems under different combinations of consecutiveness, interdigitation and rectangular constraints. We also create a virtual freeform collimator, which can form any possible segment shape by opening or closing each bixel independently, to provide a basis for comparison . We formulate the problem of minimizing beam-on time as a large-scale linear programming problem. To deal with its dimensionality, we propose a column generation approach. We demonstrate the efficacy of our approach on a set of clinical problem instances. Our results indicate that the dual MLC under consecutiveness constraint yields very similar beam-on time to a virtual freeform collimator. Our approach also provides a ranking between other collimator technologies in terms of their delivery efficiencies.

Keywords: IMRT, Multileaf Collimator, Column Generation, Linear Programming

1. Introduction

Intensity Modulated Radiation Therapy (IMRT) is a form of cancer treatment that delivers radiation beams to the patient from several directions (i.e. beam orientations) by using a linear accelerator and a collimator (Chen & Wang 2009). While linear accelerator rotates around the patient, collimator shapes the beams by moving their leaves to form different segments or apertures. This technique provides a high degree of control over the dose distribution that is received by a patient (Ehrgott et al. 2008).

IMRT treatment can be delivered either statically or dynamically. In the static approach, also called "step and shoot" technique, leaves are stationary while the radiation beam is on. In other words, the linear accelerator stops at a predetermined beam angle position, an aperture is formed and only then the radiation source is turned on (Rocha et al. 2010). In the dynamic approach, new apertures are formed while the radiation is on, so collimator leaves keep moving during the treatment (Jing et al. 2010). In this study, we focus on the static approach.

Static IMRT treatment planning process is typically composed of three phases. The first phase is called beam angle optimization (BAO). Radiation is delivered through a set of beam angles and the goal of BAO is to determine optimal beam angles (Zhang & Merritt 2006). BAO is widely studied in the literature (see Craft 2007, Lim et al. 2008, Wang et al. 2004). The second phase, fluence map optimization (FMO), aims to find an optimal fluence map (also callued intensity profile) for each beam angle. The fluence map is a nonnegative integer matrix of intensity values. The objective of this phase is to find a treatment plan that delivers the required dose of radiation to malignant tissues while healthy ones are spared (Ehrgott et al. 2008). Some approaches for solving FMO problem can be found in Zhang & Merritt (2006), Aleman et al. (2010) and Tuncel et al. (2012). In this paper, we investigate the last phase, called the leaf sequencing optimization (LSO). In LSO, the intensity matrices are decomposed into a set of deliverable apertures (i.e. segments or shape matrices) and their associated intensities so that treatment is delivered efficiently (see Cambazard et al. 2012, Taşkın et al. 2010, Taşkın & Cevik 2013). There are also some studies on approximate intensity matrix decomposition. This line of research focuses on creating a suitable treatment plan by allowing some small deviation from the given intensity matrix (see Dobler et al. 2007, Kalinowski & Kiesel 2009, Engel & Kiesel 2011, Kalinowski 2011). Dividing the IMRT treatment plan into stages and dealing with them separately may cause loss in treatment quality. Hence, some integrated approaches aim to solve multiple stages of the IMRT problem at once. For instance, direct aperture optimization (DAO) approaches integrate the FMO and LSO stages and solve the problem as a single but more complicated optimization problem (see Men et al. 2007, Men et al. 2010, Salari & Unkelbach 2013, Broderick et al. 2009, Dobler et al. 2007).

Collimator systems used in IMRT can form different geometric shapes of apertures depending on their physical capabilities. Hence, different collimator systems lead to changes in the set of feasible aperture shapes. The regular multileaf collimator (MLC) is a type of collimator that is composed of a set of leaf pairs; left and right leaves with the same sizes. In the IMRT systems with regular MLC, the linear accelerator rotates around the patient, stops at a predetermined angle and the radiation is transmitted through the aperture constructed by the regular MLC (Ahuja & Hamacher 2005). Another collimator type is the rotating MLC. It is a regular MLC with the ability of head rotation by 90°. In this system, apertures are first constructed with left-right pairs of leaves, then the MLC rotates and apertures are constructed with top-bottom pairs of leaves; or vice versa (Blin et al. 2014). Dual MLC is a kind of collimator that has two orthogonal pairs of leaves; one pair operating horizontally and the other pair simultaneously operating vertically. Hence, it is expected to construct more complex apertures (Webb 2012).

There are some common constraints that appear in collimator systems and further restrict the set of feasible aperture shapes. Consecutiveness constraint is an important restriction that applies to many collimator systems. It means that the open area constructed by the pairs of leaves should be contiguous (Ehrgott et al. 2008, Men et al. 2007). Rectangles are the simplest aperture shapes that can be formed. IMRT

can be delivered only using conventional jaws, which are devices that can only form rectangular apertures. This restriction is named as the rectangular constraint (Men et al. 2007). Interdigitation constraint is about leaves in adjacent rows. It states that the left and right leaf pairs of a row cannot overlap with the right and left pairs of the adjacent row respectively. In other words, opposing leaves of adjacent rows cannot overlap (Ehrgott et al. 2008, Kalinowski 2008). Minimum leaf separation constraint forces a minimum leaf opening in each bixel row (Chen & Wang 2009, Engelbeen & Fiorini 2010). Maximum leaf spread constraint forces a maximum distance between the edge of leftmost left and rightmost right leaf (Chen & Wang 2009, Wu et al. 2013). Tongue and groove constraint occurs due to the tongue and groove leaf arrangement of the MLCs. This arrangement is a special design for reducing the interleaf leakage. However, it may cause under-dosage. Hence, there are several studies about preventing tongue and groove effect for minimizing under-dosage (Chen & Wang 2009, Salari et al. 2011, Kalinowski 2008, Engelbeen & Fiorini 2010).

There are several studies in the literature investigating regular MLC system under different constraints and different objectives. The LSO problem of the regular MLC under consecutiveness constraint such that the total beam-on time (BOT) is minimized is widely studied (Baatar et al. 2005, Boland et al. 2004, Bortfeld et al. 1994, Kamath et al. 2003). BOT is the total time that radiation source is on and it is proportional to the sum of the aperture intensities. This problem is known to be polynomially solvable (Engel 2005, Ahuja & Hamacher 2005, Kamath et al. 2003). However, the same problem with the objective of minimizing total setup time or total treatment time is strongly NP-hard (Baatar et al. 2005). Extensive research by several researchers indicates that such NP-hard problems are very unlikely to be solved efficiently, unless significant improvements are made in the theory and practice of computational complexity. For details about NP-hardness, we refer the reader to French (1982) and Garey & Johnson (1979). Setup time occurs due to the change of apertures. Depending on the similarity of the consecutive apertures, leaf and head movements, hence setup times, between apertures change. However, modeling setup time precisely is complicated and leads to optimization models that cannot be solved within clinically feasible time limits. Therefore, setup time is usually taken as a constant value per aperture change and total setup time is estimated as a function of total number of apertures used in the decomposition (Taşkın et al. 2010, Wake et al. 2009, Langer et al. 2001). Total treatment time is estimated as the summation of beam-on time and setup time (Boland et al. 2004). There is a large number of heuristics developed for these problems such as Agazaryan & Solberg (2003) and Siochi (2007). Exact solution approaches are proposed in Ernst et al. (2009), Langer et al. (2001) with minimum number of used apertures objective and in Wake et al. (2009), Taşkın et al. (2010), Mason et al. (2012) with total treatment time objective. The LSO problem under the rectangular constraint with the minimization of total number of apertures objective is studied in Taşkın et al. (2012) and Taşkın & Cevik (2013). LSO problem under interdigitation constraint with minimum BOT objective is modelled in Kalinowski (2008). The same problem is also studied in Boland et al. (2004).

Consecutiveness and interdigitation are taken into account in the formulation of Boland et al. (2004). The BOT value is taken as a performance metric in also Li & Xing (2013).

MLCs are technologically advanced systems which are therefore difficult and expensive to build, operate and maintain (Taşkın et al. 2012). Additional features and more flexibility implies additional costs. Hence, the comparison of different MLC technologies is important to determine the value added by the additional features. There are some studies in the literature doing this comparison partially by using Monte-Carlo simulation. Anderson et al. (2006) compare several conceptual collimators, which are collimators using jaws, leaves, bars or single-bixel attenuators and a virtual freeform collimator. Freeform collimator constitutes a basis in comparison with other collimators. It can form any possible segment shape by opening or closing each bixel independently. Webb (2012) compares the regular, rotating and dual MLCs by using Monte-Carlo simulation by ignoring all constraints except the consecutiveness. Their results show that dual MLC is advantageous over the others, and rotating MLC is advantageous over the regular MLC. Blin et al. (2014) prove the hardness of the decomposition problem of an intensity matrix using rotating collimator and dual MLC. They show that these problems are NP-hard when minimizing total number of apertures or BOT.

The contribution of our study can be summarized as: (*i*) comparing the BOT performance of different collimator technologies from an optimization point of view, (*ii*) extending and unifying MLC comparison efforts present in the literature, and (*iii*) developing a common, flexible and adaptable platform for the comparison of collimator technologies.

The rest of this paper is organized as follows: In Section 2, we construct a large-scale linear programming formulation of the minimum BOT problem. To deal with its dimensionality, we revise the formulation in Section 3 and apply column generation approach. We present the results of our method on clinical data in Section 4. Finally we provide concluding remarks in Section 5.

2. General LSO Problem with Minimum BOT Objective

The input of LSO stage of IMRT treatment process is a nonnegative integer matrix of intensity values, which is called intensity matrix A. The number of rows and columns of A are respectively m and n. $A_{(mxn)}= (a_{ij})$ and a_{ij} represents the required intensity value for bixel $(i,\ j)$ $\forall i = 1, \ldots, m, j = 1, \ldots, n$. We also have the set of all feasible shape matrices, S, on hand. The cardinality of this set is represented by $\kappa = |S|$. Each shape matrix can be represented by a (0-1) matrix having the same dimensions as A. S_{ijk} indicates whether the $(i,j)^{\text{th}}$ cell of the k^{th} shape matrix among set S is exposed or not. In other words, $S_{ijk} = 1$ if bixel (i,j) is exposed in shape matrix k, and $S_{ijk} = 0$ otherwise $\forall i = 1, \ldots, m, j = 1, \ldots, n, k = 1, \ldots, \kappa$. We use X_k to represent the BOT value for shape matrix k, $\forall k = 1, \ldots, \kappa$, which is proportional to the number of monitor units associated with that shape matrix.

From now on, we will refer to the LSO problem with the objective of minimizing

total beam-on time as master problem (MP). Master problem can be formulated as follows (see Boland et al. 2004):

MP:

$$\text{minimize} \quad \sum_{k=1}^{\kappa} X_k \tag{2.1}$$

$$\text{subject to} \quad \sum_{k=1}^{\kappa} S_{ijk} X_k = a_{ij} \qquad \forall i = 1, \ldots, m, \quad j = 1, \ldots, n \tag{2.2}$$

$$X_k \geq 0 \qquad \forall k = 1, \ldots, \kappa \tag{2.3}$$

The objective function (2.1) minimizes the total beam-on time of the shape matrices. The constraint (2.2) ensures that the required amount of dosage is delivered to each bixel. Finally, the constraint (2.3) enforces non-negativity restriction of the beam-on time values.

Note that MP is a linear programming problem with just one set of constraint and κ many variables. The number of feasible shapes, κ, varies according to the physical capabilities of the used collimator system. For example, for the collimator systems that can only form rectangular shapes, two row and two column indices uniquely identify a rectangular aperture. Therefore, the number of feasible shapes is $\binom{m}{2}\binom{n}{2} = O(m^2n^2)$, which is a polynomial function of (m,n). However, κ is an exponential function of (m,n) for other cases. For instance, for Regular MLC with Consecutiveness Constraint, $\binom{n}{2}$ possible positions exist for the leaves of each row. Since the leaf position selection of a row is independent of the others, the exact number of possible shapes is $\binom{n}{2}^m$ which is an exponential function of (m,n). To deal with the problem of dealing with exponentially many variables and create a unified method for all technologies, we apply column generation approach.

3. Column Generation Approach

The MP formulation is not easy to solve because it typically has vast number of feasible shape matrices κ. Additionally, many of these feasible shapes will not be used in an optimal solution. In other words, their intensity values X_k will be zero in an optimal solution. Thus, we initially generate a subset of this set, and use that subset to solve a restricted version of the MP. Then we solve a subproblem to identify new useful shape matrices to add the subset that will improve the current solution, or conclude that the current solution is optimal. There are some studies using column generation approach in IMRT context. Boland et al. (2004) propose column generation approach to solve MP formulation for the case of using a regular MLC under interdigitation constraint. Men et al. (2007) and Men et al. (2010) use column generation algorithm to solve the direct aperture optimization problem. We refer the reader to Wolsey (1998) for details about column generation approach.

Let us first define a restricted master problem (RMP) that has only a subset of columns, i.e. shape matrices. Let $\widehat{S} \subseteq S$ and $\widehat{\kappa} \equiv \widehat{S}$. The restricted master problem can

be formulated as:

RMP:

$$\text{minimize} \quad \sum_{k=1}^{\widehat{\kappa}} X_k \tag{3.1}$$

$$\text{subject to} \quad \sum_{k=1}^{\widehat{\kappa}} S_{ijk} X_k = a_{ij} \qquad \forall i = 1, \ldots, m, \quad j = 1, \ldots, n \tag{3.2}$$

$$X_k \geq 0 \qquad \forall k = 1, \ldots, \widehat{\kappa} \tag{3.3}$$

A feasible subset of shape matrices is needed to start the column generation approach. In principle such a feasible subset can be identified by running a heuristic to obtain a feasible set of shapes. However, this approach would require availability of a heuristic for each collimator type. Therefore, we take a different approach and generate the initial subset as mxn many unit shape matrices (S_{ij} matrices with a single 1 in bixel (i, j) and 0 elsewhere, $\forall i = 1, \ldots, m, j = 1, \ldots, n$). Note that this subset always gives a feasible solution for the collimator types we investigate in this paper, and the BOT value of that solution equals the sum of the intensities ($\sum_{i=1}^{m} \sum_{j=1}^{n} a_{ij}$).

In linear programming theory, duality provides many important insights into the structure and solution of linear programming problems. For each linear programming problem, there exists a dual problem. A dual variable is associated with each original constraint. Furthermore, each original variable has a reduced cost value, which is the required amount of change in its objective coefficient in order to include it in an optimal solution. Reduced costs of all variables can be calculated by using optimal values of dual variables (Taha 2007, Winston et al. 2003). We denote the dual variables associated with the constraints (3.2) by λ_{ij}. By checking the reduced costs, we can find the most promising shape matrix for our problem to include in the RMP. Hence, a subproblem is defined to identify the shape matrix with the least reduced cost.

Given an optimal solution of RMP, subproblem (SP(λ)) can be formulated as follows:

SP(λ):

$$\text{minimize} \quad 1 - \sum_{i=1}^{m} \sum_{j=1}^{n} \lambda_{ij} S_{ij} \tag{3.4}$$

$$\text{subject to} \quad \text{S is a feasible shape matrix} \tag{3.5}$$

$$S_{ij} \in \{0, 1\} \qquad \forall i = 1, \ldots, m \quad j = 1, \ldots, n \tag{3.6}$$

The subproblem objective function (3.4) aims to find a shape matrix having the minimum reduced cost. The reduced cost is calculated by the multiplication of the dual variables λ_{ij} associated with the constraints (3.2) and the shape matrix S_{ij} (Taha 2007, Winston et al. 2003). Note that RMP's structure does not depend on the collimator system. However, each collimator type leads to a different SP(λ) feasible region. Hence, constraint (3.5) means ensuring the feasibility of the shape matrix for the conditions of the investigated case, and needs to be defined precisely for each case.

If optimal objective value of SP(λ) is nonnegative, then the current solution to the RMP optimally solves the original formulation MP as well. If optimal objective value of SP(λ) is negative, we add the new column to the RMP and solve it again (Wolsey 1998). In the following sections we explain the SP(λ) of the cases of our concern and discuss their solution procedures.

3.1. Subproblem for Regular MLC with Consecutiveness Constraint

It is known that the LSO problem of regular MLC under consecutiveness constraint with the objective of minimizing BOT can be solved in polynomial time, and there are various algorithms for solving that problem as stated in Section 1. Since the aim of our study is to construct a common basis for comparison, we investigate the use of column generation method for this case also.

We observe that SP(λ) of this case is decomposable by each bixel row. Hence, an optimal solution under consecutiveness constraint can be found by first finding an optimal leaf setting for each row, then combining these leaf settings to form an optimal aperture shape. An optimal leaf setting for each row can be found by a single pass algorithm similar to Romeijn et al. (2005). According to the algorithm to find the leaf positions of a single row i, we sum $-\lambda_{ij}$ terms cumulatively over index j. Since our aim is to minimize the cumulative $-\lambda_{ij}$ sum in the SP(λ) objective (3.4), we save the maximum value of the cumulative sum encountered so far. To eliminate those big $-\lambda_{ij}$ terms, we pull the left leaf to the j^{th} index, where we obtain the maximum cumulative sum value. In this way, we close the bixels with big $-\lambda_{ij}$ values. Then we compare the maximum with the cumulative sum value. The position that we obtain the minimum difference between these two values gives the optimal right leaf position. Hence, the algorithm finds the optimal leaf positions for a row. We apply this single pass algorithm to all rows, then combine the best leaf settings for each row to obtain an optimal aperture shape. The complexity of this algorithm for a single row is O(n). Since the algorithm needs to be executed for each row to form an optimal aperture shape, the overall complexity is O(mn).

3.2. Subproblem for Regular MLC with Interdigitation Constraint

Interdigitation constraint is related to adjacent rows, therefore the problem is not separable with respect to rows as the previous case. To solve SP(λ) in this case, we define a shortest path network as it is done in Men et al. (2007) and Boland et al. (2004). The nodes are defined by each potential leaf setting in each bixel row, and represented by (i, c_1, c_2) where i is the row index ($i \in \{1, \ldots, m\}$), c_1 and c_2 are the potential left and right leaf positions ($c_1 \in \{0, \ldots, n\}$, $c_2 \in \{1, \ldots, n+1\}$). In addition to these, we add a source and a sink node to represent the top and bottom of the aperture. To satisfy interdigitation restriction, we define an arc from node (i, c_1, c_2) to the next layer node of ($i+1$, c_1', c_2') if and only if $c_1' \leq c_2 - 1$ and $c_2' \geq c_1 + 1$. For example, a complete shape matrix network of a 2x2 intensity matrix under interdigitation constraint is given

in Figure 1. Three example shape matrices are given from that complete network in

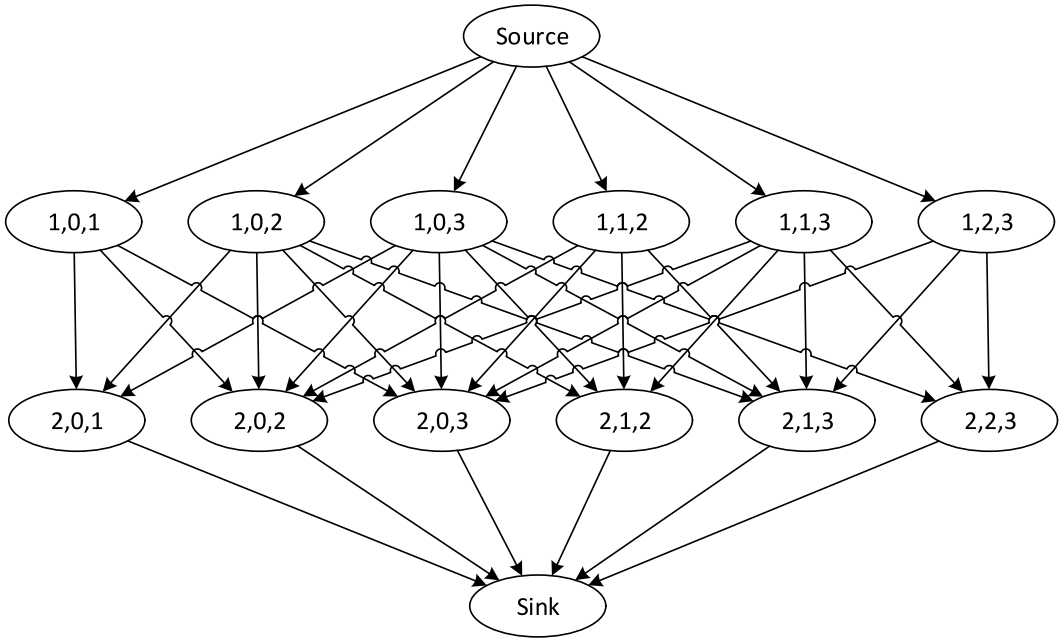

Figure 1. The complete shape matrix network of a 2x2 matrix.

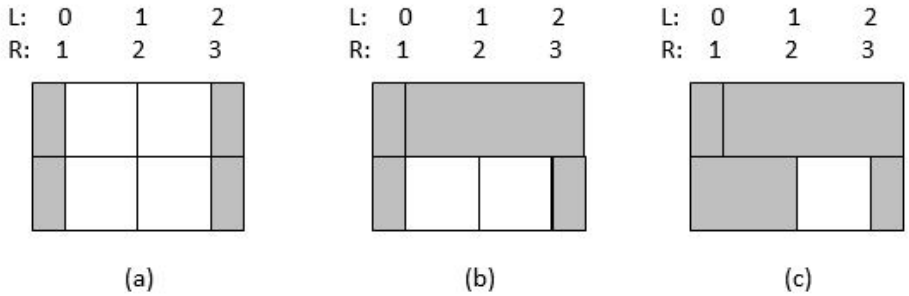

Figure 2. Shape matrices having leaf positions (a) (1,0,3)-(2,0,3), (b) (1,0,1)-(2,0,3), (c) (1,0,1)-(2,1,3).

Figure 2. Possible left and right leaf positions are shown respectively as "L" and "R" on top of the matrices. The example matrix on Figure 2 (a) corresponds to path $(Source) \rightarrow$ (1,0,3) $\rightarrow$ (2,0,3) $\rightarrow (Sink)$. The matrix on Figure 2 (b) represents the path of $(Source)$ $\rightarrow$ (1,0,1) $\rightarrow$ (2,0,3) $\rightarrow (Sink)$. Both of these paths exist in the network of Figure 1, since they satisfy the interdigitation restriction. However, the path of $(Source) \rightarrow$ (1,0,3) $\rightarrow$ (2,1,3) $\rightarrow (Sink)$ of the matrix (c) does not exist in the network, because second left leaf overpasses the first right leaf, which violates interdigitation constraint. Furthermore, we set arc costs as the sum of all objective function coefficients corresponding to the exposed bixels $(-\sum_{j=c_1+1}^{c_2-1} \lambda_{ij})$ of the shape matrix. With this construction, a shortest path from source to sink node gives a shape matrix with the least reduced cost.

In each layer of the network, there are $\binom{n+1}{2}$ many nodes. The total number of nodes

is $\left[\frac{m(n+1)(n+2)}{2}+2\right]=\mathrm{O}(mn^2)$. The total number of arcs is $\mathrm{O}(mn^3)$. Thus, complexity of the overall shortest path algorithm is $\mathrm{O}(mn^3)$.

3.3. Subproblem for Regular MLC with Rectangular Constraint

To form a rectangle, two row selections (r_1, r_2) and two column selections (c_1, c_2) need to be made among the possible m and n options. Suppose that which rows are exposed in the rectangle aperture is known in advance, then the SP(λ) under rectangular constraint becomes equivalent to the SP(λ) under consecutiveness investigated in Section 3.1. There are $\mathrm{O}(m^2)$ possible row selections. Hence, a rectangular aperture can be formed by applying a slightly modified single pass algorithm for all $\mathrm{O}(m^2)$ possible row selections and selecting the minimum one (Men et al. 2007). New coefficients used in the algorithm are $-\sum_{i=r_1}^{r_2}\lambda_{ij}$. This version of single pass algorithm has complexity of $\mathrm{O}(m^2n)$. However, this can be adjusted carefully by checking $\min\{m,n\}$. Since a rectangle is consecutive in terms of both rows and columns, if $n<m$, then we apply single pass algorithm for all $\mathrm{O}(n^2)$ possible column selections. With this point of view, the complexity of the solution algorithm is $\mathrm{O}\big(\min\{m,n\}^2\max\{m,n\}\big)$.

Note that rotating a rectangular aperture yields another rectangular aperture. Hence, we do not investigate rotating MLC with rectangular constraint.

3.4. Subproblem for Rotating MLC with Consecutiveness Constraint

In rotating MLC, either a row- or column-consecutive shape matrix is constructed during the treatment. Hence, either row- or column-consecutiveness constraint must be active in the feasible region of the SP(λ). To solve that problem, we apply our single pass algorithm twice; once to find a row-consecutive shape matrix as in Section 3.1 and once to find a column-consecutive shape matrix. We then compare the two shape matrices and select the one with the smaller objective value as the SP(λ) optimal solution. The overall complexity of the algorithm is $\mathrm{O}(mn)$.

3.5. Subproblem for Rotating MLC with Interdigitation Constraint

Similar to Section 3.4, we apply interdigitation either row-based or column-based in rotating MLC. To solve the SP(λ), we define two similar shortest path problems: The first one is over columns as it is done in Section 3.2, and, the second one is defined over rows. We solve those two problems and generate two shape matrices. The one having the minimum objective value among these two shape matrices determines an optimal solution to the SP(λ). The complexity of this algorithm is $\mathrm{O}(mn^3+nm^3)$, which is $\mathrm{O}(\max\{mn^3,nm^3\})$. mn^3 term comes from the row based interdigitation part of the algorithm as in Section 3.2 and nm^3 is adapted for the column based interdigitation part.

3.6. Subproblem for Dual MLC with Consecutiveness Constraint

In dual MLC, there are two separate orthogonal layers. We call the left-right leaf setting as the horizontal layer and top-bottom leaf setting as the vertical layer. Note that LSO problem of the dual MLC is NP-hard when minimizing BOT (Blin et al. 2014). Hence, we formulate the SP(λ) corresponding to dual MLC as an integer programming problem.

Since an aperture is formed by the combination of layers, two layers must be represented in the formulation and the shape matrix must be constructed from their intersection. We define four types of decision variables to represent the leaf positions. These decision variables are equal to 1 if bixel (i, j) is covered by the corresponding leaf, and 0 otherwise, $\forall i = 1, \ldots, m, j = 1, \ldots, n$. L_{ij} represents the left leaf, R_{ij} the right leaf, T_{ij} the top leaf and B_{ij} the bottom leaf. We also have two more decision variables to represent whether bixel (i, j) is exposed vertically, V_{ij}, or horizontally, H_{ij}, $\forall i = 1, \ldots, m, j = 1, \ldots, n$.

We formulate the SP(λ) as:

$$\min \quad \sum_{i=1}^{m} \sum_{j=1}^{n} -\lambda_{ij} S_{ij} \tag{3.7}$$

$$\text{s.t.} \quad S_{ij} \geq V_{ij} + H_{ij} - 1 \qquad \forall i = 1, \ldots, m \qquad \forall j = 1, \ldots, n \tag{3.8}$$

$$S_{ij} \leq V_{ij} \qquad \forall i = 1, \ldots, m \qquad \forall j = 1, \ldots, n \tag{3.9}$$

$$S_{ij} \leq H_{ij} \qquad \forall i = 1, \ldots, m \qquad \forall j = 1, \ldots, n \tag{3.10}$$

$$L_{ij} + R_{ij} + H_{ij} = 1 \qquad \forall i = 1 \ldots, m \qquad \forall j = 1, \ldots, n \tag{3.11}$$

$$L_{ij} \leq L_{i(j-1)} \qquad \forall i = 1, \ldots, m \qquad \forall j = 2, \ldots, n \tag{3.12}$$

$$R_{ij} \leq R_{i(j+1)} \qquad \forall i = 1, \ldots, m \qquad \forall j = 1, \ldots, n-1 \tag{3.13}$$

$$T_{ij} + B_{ij} + V_{ij} = 1 \qquad \forall i = 1, \ldots, m \qquad \forall j = 1, \ldots, n \tag{3.14}$$

$$T_{ij} \leq T_{(i-1)j} \qquad \forall i = 2, \ldots, m \qquad \forall j = 1, \ldots, n \tag{3.15}$$

$$B_{ij} \leq B_{(i+1)j} \qquad \forall i = 1, \ldots, m-1 \qquad \forall j = 1, \ldots, n \tag{3.16}$$

$$L_{ij}, R_{ij}, T_{ij}, B_{ij} \in \{0, 1\} \qquad \forall i = 1, \ldots, m \qquad \forall j = 1, \ldots, n \tag{3.17}$$

$$S_{ij}, V_{ij}, H_{ij} \geq 0 \qquad \forall i = 1, \ldots, m \qquad \forall j = 1, \ldots, n \tag{3.18}$$

The constraint (3.8) ensures that the bixel (i,j) is exposed if it is open in both horizontal and vertical layers. The constraints (3.9) and (3.10) ensure that if the bixel (i,j) is blocked in one of the layers, then it must be blocked in the shape matrix. The constraints (3.11) and (3.14) state that bixel (i,j) can either be exposed horizontally (resp. vertically) or covered by left (resp. top) or right (resp. bottom) leaf. The constraints (3.12) and (3.13) enforce that if bixel (i,j) is covered by the left leaf (resp. right leaf), then the left of that bixel (resp. right of that bixel) must also be covered by the same leaf. Constraints (3.15) and (3.16) apply the corresponding restrictions on top and bottom leaves. Finally, constraints (3.17) and (3.18) define variable types. Note that S_{ij}, V_{ij} and H_{ij} variables do not need to be defined as binary, since they will take binary values if L_{ij}, R_{ij}, T_{ij} and B_{ij} variables are binary.

3.7. Subproblem for Freeform Collimator

Freeform collimator is a theoretical collimator that can form any possible aperture shape by opening or closing each bixel independently. Therefore, the SP(λ) of the freeform collimator has no constraints. As solution approach, we employ a simple logic. If $-\lambda_{ij} < 0$, then $S_{ij} = 1$; meaning that bixel (i,j) is open. Else, $S_{ij} = 0$; meaning that bixel (i,j) is closed. Since any segment shape is possible, this simple algorithm gives an optimal solution to the SP(λ) of freeform collimator in O(mn) time.

4. Results

We have implemented our column generation algorithm for all cases, using CPLEX 12.5, running on a Windows 7 PC with a 3.60 GHz CPU and 32 GB RAM. Our test problem instances are gathered from the treatment plans of eleven head-and-neck cancer patients. Each patient is treated using five beam angles. First 25 of this data set have been used in various articles such as Taşkın et al. (2012), Taşkın & Cevik (2013), Mason et al. (2012), Taşkın et al. (2010) and Ernst et al. (2009). The maximum intensity value for all 55 instances is $L = 20$.

The BOT results for different collimator types can be found at Table 1. The test instance characteristics are summarized in the first three columns of the table. The column "$Name$" shows the instance name. "m" shows the number of rows and "n" the number of columns of the given intensity matrix. "$Free$" represents the BOT value of virtual freeform collimator (Section 3.7), "$Dual$" represents the BOT value of dual MLC under consecutiveness constraint (Section 3.6), "Reg_Cons" regular MLC under consecutiveness constraint (Section 3.1), "Reg_Int" regular MLC under interdigitation constraint (Section 3.2), "$Rect$" collimators that can only form rectangular shapes (Section 3.3), "Rot_Cons" rotating MLC under consecutiveness constraint (Section 3.4) and "Rot_Int" rotating MLC under interdigitation constraint (Section 3.5), respectively. Freeform collimator always yields the minimum BOT value as expected. Therefore, for each case we find the ratio of BOT value to freeform BOT value and call those proportions "τ_{Free}," "τ_{Dual}," "τ_{Reg_Cons}," "τ_{Reg_Int}," "τ_{Rect}," "τ_{Rot_Cons}" and "τ_{Rot_Int}," respectively. The last rows of the Table 1, named as "$min\ \tau$," "$avg\ \tau$" and "$max\ \tau$," shows the minimum, average and maximum ratios for the collimator technologies to the freeform collimator.

Table 1 indicates that the virtual freeform collimator yields the smallest BOT results among all collimators and the minimum possible BOT value is $L = 20$ as expected. Furthermore, since rectangles are very simple shapes, it is also not surprising that the collimators that can only form rectangular shapes have the largest BOT values. On the average, the closest value to minimum BOT found by rectangular collimators is 8.61 times the minimum BOT value found by freeform collimator. However, it is interesting to see that the dual MLC matches the freeform BOT values for 51 out of 55 instances.

It is not easy to evaluate the differences in the efficiency of using different collimator

Table 1. Beam-on time for different collimator types.

Name	*m*	*n*	*Free*	τ_{Free}	*Dual*	τ_{Dual}	*Reg_Cons*	τ_{Reg_Cons}	*Reg_Int*	τ_{Reg_Int}	*Rect*	τ_{Rect}	*Rot_Cons*	τ_{Rot_Cons}	*Rot_Int*	τ_{Rot_Int}
case1beam1	15	14	20	1	20.00	1.00	40	2.00	51	2.55	176.00	8.80	25.00	1.25	34.00	1.70
case1beam2	11	15	20	1	20.00	1.00	34	1.70	37	1.85	121.00	6.05	20.00	1.00	21.50	1.08
case1beam3	15	15	20	1	20.00	1.00	31	1.55	36	1.80	147.00	7.35	20.00	1.00	28.00	1.40
case1beam4	15	15	20	1	20.00	1.00	33	1.65	34	1.70	136.00	6.80	24.00	1.20	27.00	1.35
case1beam5	11	15	20	1	20.00	1.00	34	1.70	40	2.00	115.00	5.75	20.00	1.00	25.00	1.25
case2beam1	18	20	20	1	20.00	1.00	34	1.70	40	2.00	194.00	9.70	20.50	1.03	29.00	1.45
case2beam2	17	19	20	1	20.33	1.02	41	2.05	48	2.40	207.00	10.35	20.33	1.02	27.65	1.38
case2beam3	18	18	20	1	20.00	1.00	49	2.45	52	2.60	237.00	11.85	23.00	1.15	32.00	1.60
case2beam4	18	18	20	1	20.00	1.00	51	2.55	52	2.60	258.00	12.90	20.00	1.00	27.88	1.39
case2beam5	17	18	20	1	20.00	1.00	39	1.95	40	2.00	207.00	10.35	21.00	1.05	26.50	1.33
case3beam1	22	17	20	1	20.33	1.02	41	2.05	43	2.15	266.00	13.30	26.50	1.33	27.60	1.38
case3beam2	15	19	20	1	20.00	1.00	46	2.30	49	2.45	151.00	7.55	20.00	1.00	21.43	1.07
case3beam3	20	17	20	1	20.00	1.00	49	2.45	55	2.75	278.00	13.90	27.67	1.38	31.17	1.56
case3beam4	19	17	20	1	20.00	1.00	43	2.15	57	2.85	287.00	14.35	23.00	1.15	28.40	1.42
case3beam5	15	19	20	1	20.00	1.00	34	1.70	51	2.55	182.00	9.10	20.00	1.00	27.78	1.39
case4beam1	19	22	20	1	20.67	1.03	40	2.00	62	3.10	275.00	13.75	23.00	1.15	42.50	2.13
case4beam2	13	24	20	1	20.00	1.00	69	3.45	73	3.65	232.00	11.60	21.50	1.08	27.00	1.35
case4beam3	18	23	20	1	20.00	1.00	39	1.95	40	2.00	189.00	9.45	24.00	1.20	26.00	1.30
case4beam4	17	23	20	1	20.00	1.00	42	2.10	51	2.55	235.00	11.75	20.43	1.02	28.00	1.40
case4beam5	12	24	20	1	20.00	1.00	73	3.65	77	3.85	260.00	13.00	21.50	1.08	27.06	1.35
case5beam1	15	16	20	1	20.00	1.00	26	1.30	41	2.05	158.00	7.90	20.00	1.00	27.50	1.38
case5beam2	13	17	20	1	20.00	1.00	41	2.05	65	3.25	156.00	7.80	20.00	1.00	25.57	1.28
case5beam3	14	16	20	1	20.00	1.00	34	1.70	38	1.90	180.00	9.00	20.00	1.00	25.33	1.27
case5beam4	14	16	20	1	20.00	1.00	40	2.00	42	2.10	145.00	7.25	20.50	1.03	23.33	1.17
case5beam5	12	17	20	1	20.00	1.00	44	2.20	51	2.55	147.00	7.35	20.00	1.00	23.00	1.15
case6beam1	13	15	20	1	20.00	1.00	36	1.80	40	2.00	129.00	6.45	26.00	1.30	27.50	1.38
case6beam2	8	15	20	1	20.00	1.00	33	1.65	45	2.25	94.00	4.70	20.00	1.00	20.00	1.00
case6beam3	10	17	20	1	20.00	1.00	45	2.25	49	2.45	160.00	8.00	23.50	1.18	26.50	1.33
case6beam4	10	16	20	1	20.00	1.00	35	1.75	53	2.65	150.00	7.50	21.33	1.07	28.00	1.40
case6beam5	8	15	20	1	20.00	1.00	35	1.75	40	2.00	88.00	4.40	20.00	1.00	23.00	1.15
case7beam1	16	15	20	1	20.00	1.00	39	1.95	66	3.30	256.00	12.80	25.50	1.28	47.00	2.35
case7beam2	14	17	20	1	20.00	1.00	38	1.90	43	2.15	130.00	6.50	20.00	1.00	22.50	1.13
case7beam3	15	16	20	1	20.00	1.00	48	2.40	49	2.45	161.00	8.05	23.00	1.15	26.00	1.30
case7beam4	15	16	20	1	20.00	1.00	31	1.55	32	1.60	139.33	6.97	20.00	1.00	21.25	1.06
case7beam5	17	17	20	1	20.00	1.00	41	2.05	42	2.10	149.00	7.45	20.00	1.00	23.33	1.17
case8beam1	17	14	20	1	20.00	1.00	30	1.50	34	1.70	173.00	8.65	21.50	1.08	32.00	1.60
case8beam2	15	15	20	1	20.00	1.00	38	1.90	52	2.60	111.00	5.55	20.00	1.00	21.50	1.08
case8beam3	17	14	20	1	20.00	1.00	35	1.75	36	1.80	173.67	8.68	23.50	1.18	26.00	1.30
case8beam4	16	14	20	1	20.00	1.00	33	1.65	39	1.95	144.00	7.20	20.00	1.00	23.50	1.18
case8beam5	15	15	20	1	20.00	1.00	38	1.90	39	1.95	119.00	5.95	21.00	1.05	28.00	1.40
case9beam1	14	13	20	1	20.00	1.00	33	1.65	44	2.20	154.00	7.70	24.50	1.23	26.25	1.31
case9beam2	13	14	20	1	20.00	1.00	35	1.75	51	2.55	135.00	6.75	20.00	1.00	26.00	1.30
case9beam3	14	13	20	1	20.00	1.00	34	1.70	35	1.75	127.00	6.35	20.00	1.00	25.00	1.25
case9beam4	14	14	20	1	20.00	1.00	38	1.90	39	1.95	139.00	6.95	20.00	1.00	23.07	1.15
case9beam5	14	14	20	1	20.00	1.00	42	2.10	47	2.35	134.00	6.70	20.00	1.00	26.00	1.30
case10beam1	17	25	20	1	20.57	1.03	46	2.30	78	3.90	348.00	17.40	25.75	1.29	34.75	1.74
case10beam2	10	26	20	1	20.00	1.00	66	3.30	78	3.90	179.00	8.95	20.67	1.03	29.00	1.45
case10beam3	18	24	20	1	20.00	1.00	45	2.25	47	2.35	184.00	9.20	20.00	1.00	22.00	1.10
case10beam4	15	24	20	1	20.00	1.00	44	2.20	57	2.85	211.00	10.55	20.00	1.00	21.25	1.06
case10beam5	13	27	20	1	20.00	1.00	48	2.40	54	2.70	196.00	9.80	20.00	1.00	23.25	1.16
case11beam1	12	14	20	1	20.00	1.00	39	1.95	39	1.95	168.00	8.40	25.00	1.25	26.50	1.33
case11beam2	12	13	20	1	20.00	1.00	27	1.35	27	1.35	103.50	5.18	20.00	1.00	20.00	1.00
case11beam3	11	13	20	1	20.00	1.00	29	1.45	29	1.45	93.00	4.65	20.00	1.00	20.00	1.00
case11beam4	12	13	20	1	20.00	1.00	27	1.35	27	1.35	106.00	5.30	20.00	1.00	20.00	1.00
case11beam5	9	14	20	1	20.00	1.00	29	1.45	29	1.45	82.00	4.10	20.00	1.00	20.00	1.00
min τ				1		1.00		1.30		1.35		4.10		1.00		1.00
avg τ				1		1.00		1.99		2.33		8.61		1.08		1.32
max τ				1		1.03		3.65		3.90		17.40		1.38		2.35

technologies from Table 1. Therefore, to visualize the results, we compare them by using a performance profile chart (Dolan & Moré 2002). We use BOT value of the treatment as the performance metric. Figure 3 shows $P_s(\tau)$, which is the percentage of times that collimator system s can find BOT values that are within factor τ of the minimum BOT. For example, if we choose $\tau = 2$ from Table 1, for "*Rot_Int*," 53 out of 55 instances have $\tau \leq 2$, hence $P_s(\tau = 2) = 0.96$. In other words, "*Rot_Int*" can find BOT values in between 20 and 40 ($= 2 \times 20$) in 96% of the cases. Similarly if we choose $\tau = 3$, for "*Reg_Int*," 48 out of 55 instances have $\tau \leq 3$, hence $P_s(\tau = 3) = 0.87$. That is to say that "*Reg_Int*" can find BOT values in between 20 and 60 ($= 3 \times 20$) in 87%

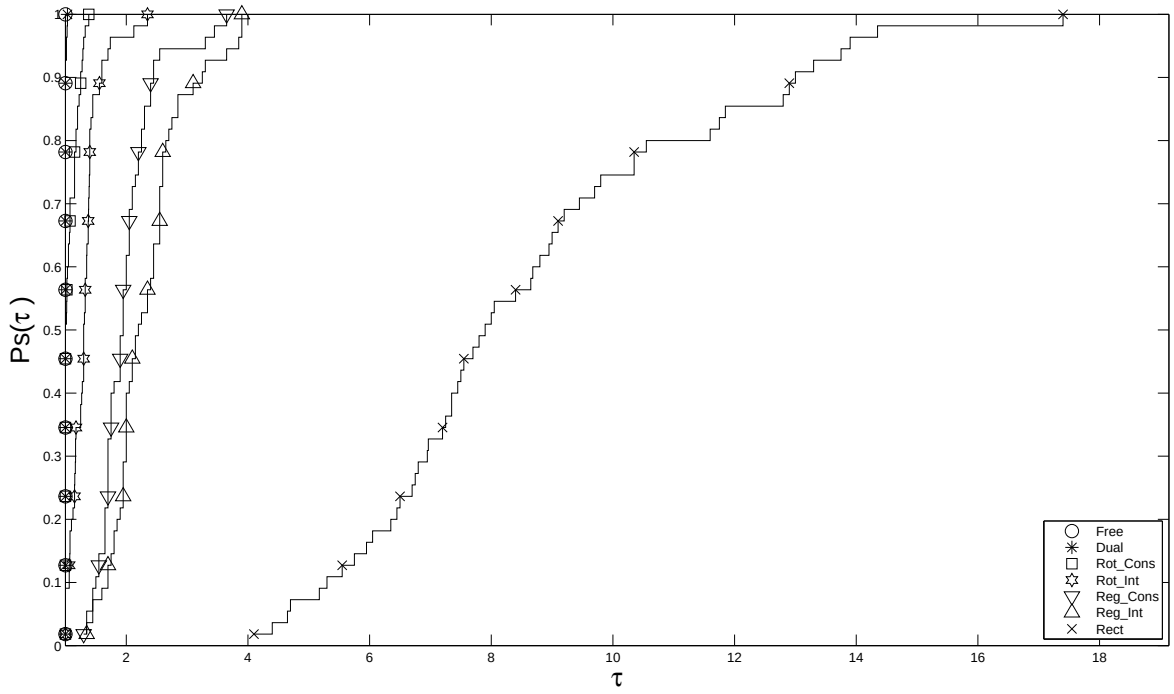

Figure 3. The performance profile chart for the BOT values used as performance metric.

of the cases. Note that $P_s(1)$ shows the percentage of times that collimator system s can find the overall minimum BOT value. From $\tau = 1$ line of the Figure 3, we see that all of the minimum BOT values are found by the freeform collimator, which is expected. Dual MLC performs very similar to freeform collimator. Then rotating MLC under consecutiveness constraint follows them in terms of BOT efficiency. It matches the minimum for 28 instances. Rotating MLC under interdigitation constraint matches the minimum for only 5 instances and the rest of the collimator systems could not find the overall minimum BOT value for any of the instances. The worst performance on the BOT values is obtained by the regular MLC under rectangular constraint. As it can be seen from Table 1, its minimum deviation from the minimum BOT value is 4.10, which is larger than the maximum deviation of other collimators.

To investigate the mean and median behaviour of the results, we create a box plot in Figure 4. In the box plot, upper and lower edges of the boxes represent the 25% and 75% quartiles of the data. The lines extending vertically from the boxes indicates variability outside the quartiles. The top and the bottom of the lines show the maximum and minimum data value excluding outliers. Outliers are plotted with "x" symbol. If the distance of the data point from the box exceeds the difference between the 25% and 75% quartiles of the data, the point is labeled as outlier. The circles in the boxes show the mean values and the lines show the median values of the instance results. Dual MLC and freeform collimator have the minimum median, and almost identical mean values. Rotating MLC under consecutiveness gives similar results as them, but it has

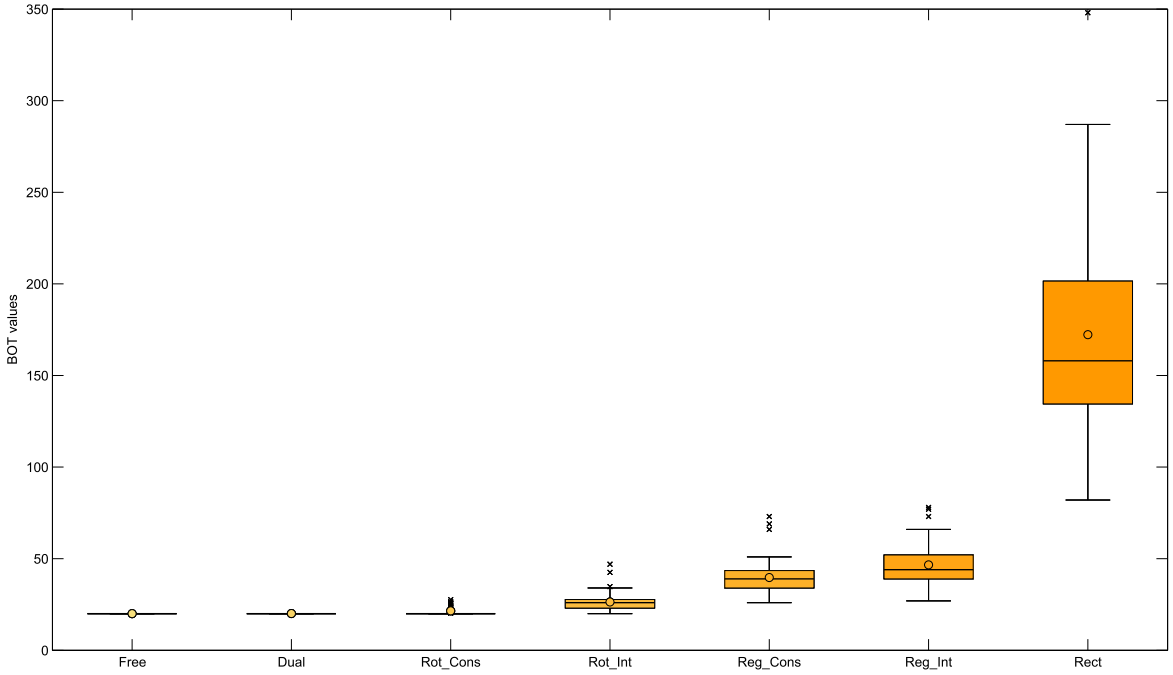

Figure 4. Box plot for the BOT results of the cases.

several outliers. The significant difference between the results of regular MLC under rectangular constraint and the others is clearly visible in Figure 4. The minimum value found by the regular MLC under rectangular constraint is larger than the maximum value found by the others. Additionally, mean value of regular MLC under rectangular constraint is higher than the median value due to the presence of an extreme outlier (case10beam1, whose BOT value is 348).

5. Summary and Conclusion

In this paper, we investigated the leaf sequencing optimization problem with minimum beam-on time objective. We compared the efficiency of using different collimator technologies under different restrictions. We focused on the testing of regular, rotating and dual multileaf collimator systems under different combinations of consecutiveness, interdigitation and rectangular constraints and a virtual freeform collimator. Our aim was to generate a comparison basis for them and formulate a general leaf sequencing optimization problem with minimum beam on time objective. We applied column generation approach to deal with the dimensionality of the formulation. In our column generation procedure, the subproblem structure changes depending on the used machinery. Hence, we generated seven different subproblems to solve each collimator case.

Our tests on clinical data show that the dual MLC under consecutiveness constraint acts almost as well as a virtual freeform collimator in terms of beam-on time values. This result is due to the fact that dual MLC is the most flexible collimator system after

the freeform collimator. Based on our computational study, the efficiency ranking is as follows; rotating MLC under consecutiveness, rotating MLC under interdigitation, regular MLC under consecutiveness, regular MLC under interdigitation and, finally, regular MLC under rectangular constraint. Collimators that can only form rectangular shapes yield very high results in terms of beam-on time. According to our analysis, it can be concluded that as the complexity of the collimator system increases and the restrictions on the system decreases, lower beam-on time results are obtained, and the dual MLC is very close to the ultimate limit.

Note that our main goal in this paper is to compare various MLCs from a delivery efficiency point of view. To this end, we focused on the leaf sequencing optimization stage of IMRT, where we quantified delivery efficiency by calculating the required BOT to deliver a given fluence map via various MLCs. Our approach can be extended to compare various MLCs in terms of the plan generated via Direct Machine Parameter Optimization (DMPO)/Direct Aperture Optimization (DAO), which also allow the doctor's objectives to be incorporated into the optimization model. Similarly, approximate intensity matrix decomposition approaches aim to balance dose delivery precision and efficiency. Our approach can also be extended to compare MLCs within an approximate decomposition setting as a future research direction.

References

Agazaryan N & Solberg T D 2003 'Segmental and Dynamic Intensity-Modulated Radiotherapy Delivery Techniques for Micro-Multileaf Collimator' *Medical Physics* **30**(7), 1758–1767.

Ahuja R K & Hamacher H W 2005 'A Network Flow Algorithm to Minimize Beam-On Time for Unconstrained Multileaf Collimator Problems in Cancer Radiation Therapy' *Networks* **45**(1), 36–41.

Aleman D M, Glaser D, Romeijn H E & Dempsey J F 2010 'Interior Point Algorithms: Guaranteed Optimality for Fluence Map Optimization in IMRT' *Physics in Medicine and Biology* **55**(18), 5467.

Anderson J, Symonds-Tayler R & Webb S 2006 'Investigating the Fundamentals of IMRT Decomposition using Ten Simple Collimator Models' *Physics in Medicine and Biology* **51**(9), 2225.

Baatar D, Hamacher H W, Ehrgott M & Woeginger G J 2005 'Decomposition of Integer Matrices and Multileaf Collimator Sequencing' *Discrete Applied Mathematics* **152**(1), 6–34.

Blin G, Morel P, Rizzi R & Vialette S 2014 'Towards Unlocking the Full Potential of Multileaf Collimators' *SOFSEM 2014: Theory and Practice of Computer Science* p. 138.

Boland N, Hamacher H W & Lenzen F 2004 'Minimizing Beam-On Time in Cancer Radiation Treatment using Multileaf Collimators' *Networks* **43**(4), 226–240.

Bortfeld T R, Kahler D L, Waldron T J & Boyer A L 1994 'X-ray field compensation with multileaf collimators' *International Journal of Radiation Oncology, Biology and Physics* **28**(3), 723–730.

Broderick M, Leech M & Coffey M 2009 'Direct Aperture Optimization as a Means of Reducing the Complexity of Intensity Modulated Radiation Therapy Plans' *Radiation Oncology* **4**(8), 1–7.

Cambazard H, O'Mahony E & O'Sullivan B 2012 'A Shortest Path-Based Approach to the Multileaf Collimator Sequencing Problem' *Discrete Applied Mathematics* **160**(1), 81–99.

Chen D Z & Wang C 2009 'Algorithms for Geometric Problems in Intensity-Modulated Radiation Therapy' *RIMS Kokyuroku* **1641**, 45–67.

Craft D 2007 'Local Beam Angle Optimization with Linear Programming and Gradient Search' *Physics in Medicine and Biology* **52**(7), N127.

Dobler B, Pohl F, Bogner L & Koelbl O 2007 'Comparison of direct machine parameter optimization versus fluence optimization with sequential sequencing in IMRT of hypopharyngeal carcinoma' *Radiation Oncology* **2**(1), 33.

Dolan E D & Moré J J 2002 'Benchmarking Optimization Software with Performance Profiles' *Mathematical Programming* **91**(2), 201–213.

Ehrgott M, Güler Ç, Hamacher H W & Shao L 2008 'Mathematical Optimization in Intensity Modulated Radiation Therapy' *4OR* **6**(3), 199–262.

Engel K 2005 'A New Algorithm for Optimal Multileaf Collimator Field Segmentation' *Discrete Applied Mathematics* **152**(1), 35–51.

Engel K & Kiesel A 2011 'Approximated matrix decomposition for IMRT planning with multileaf collimators' *OR Spectrum* **33**(1), 149–172.

Engelbeen C & Fiorini S 2010 The Segmentation Problem in Radiation Therapy PhD thesis Université Libre de Bruxelles.

Ernst A T, Mak V H & Mason L R 2009 'An Exact Method for the Minimum Cardinality Problem in the Treatment Planning of Intensity-Modulated Radiotherapy' *INFORMS Journal on Computing* **21**(4), 562–574.

French S 1982 *Sequencing and scheduling: an introduction to the mathematics of the job-shop* Vol. 683 Ellis Horwood Chichester.

Garey M R & Johnson D S 1979 'Computers and intractability'.

Jing J, Cao R, Pei X, Wu Y, Li G & Lin H 2010 'Optimization of Multileaf Collimator Leaf Sequences based on Multiple Algorithms' *in* 'Bioinformatics and Biomedical Engineering (iCBBE), 2010 4th International Conference on' IEEE pp. 1–4.

Kalinowski T 2008 'Reducing the Tongue-and-Groove Underdosage in MLC Shape Matrix Decomposition' *Algorithmic Operations Research* **3**(2).

Kalinowski T 2011 'A Minimum Cost Flow Formulation for Approximated MLC Segmentation' *Networks* **57**(2), 135–140.

Kalinowski T & Kiesel A 2009 'Approximated MLC shape matrix decomposition with interleaf collision constraint' *Algorithmic Operations Research* **4**(1).

Kamath S, Sahni S, Li J, Palta J & Ranka S 2003 'Leaf Sequencing Algorithms for Segmented Multileaf Collimation' *Physics in Medicine and Biology* **48**(3), 307.

Langer M, Thai V & Papiez L 2001 'Improved Leaf Sequencing Reduces Segments or Monitor Units Needed to Deliver IMRT using Multileaf Collimators' *Medical Physics* **28**(12), 2450–2458.

Li R & Xing L 2013 'An adaptive planning strategy for station parameter optimized radiation therapy (SPORT): Segmentally boosted VMAT' *Medical physics* **40**(5).

Lim G J, Choi J & Mohan R 2008 'Iterative Solution Methods for Beam Angle and Fluence Map Optimization in Intensity Modulated Radiation Therapy Planning' *OR Spectrum* **30**(2), 289–309.

Mason L R, Mak-Hau V H & Ernst A T 2012 'An Exact Method for Minimizing the Total Treatment Time in Intensity-Modulated Radiotherapy' *Journal of the Operational Research Society* **63**(10), 1447–1456.

Men C, Jia X & Jiang S B 2010 'GPU-Based Ultra-Fast Direct Aperture Optimization for Online Adaptive Radiation Therapy' *Physics in Medicine and Biology* **55**(15), 4309.

Men C, Romeijn H E, Taşkın Z C & Dempsey J F 2007 'An Exact Approach to Direct Aperture Optimization in IMRT Treatment Planning' *Physics in Medicine and Biology* **52**(24), 7333.

Rocha H, Dias J, Ferreira B & Lopes M 2010 'Towards Efficient Transition from Optimized to Delivery Fluence Maps in Inverse Planning of Radiotherapy Design'.

Romeijn H E, Ahuja R K, Dempsey J F & Kumar A 2005 'A Column Generation Approach to Radiation Therapy Treatment Planning using Aperture Modulation' *SIAM Journal on Optimization* **15**(3), 838–862.

Salari E, Men C & Romeijn H E 2011 'Accounting for the Tongue-and-Groove Effect using a Robust Direct Aperture Optimization Approach' *Medical Physics-New York-Institute of Physics* **38**(3), 1266.

Salari E & Unkelbach J 2013 'A Column-Generation-Based Method for Multi-Criteria Direct Aperture Optimization' *Physics in Medicine and Biology* **58**(3), 621.

Siochi R A C 2007 'Variable Depth Recursion Algorithm for Leaf Sequencing' *Medical Physics* **34**(2), 664–672.

Taha H A 2007 *Operations research: an introduction* Pearson/Prentice Hall.

Taşkın Z C & Cevik M 2013 'Combinatorial Benders Cuts for Decomposing IMRT Fluence Maps using Rectangular Apertures' *Computers & Operations Research* **40**(9), 2178–2186.

Taşkın Z C, Smith J C & Romeijn H E 2012 'Mixed-Integer Programming Techniques for Decomposing IMRT Fluence Maps using Rectangular Apertures' *Annals of Operations Research* **196**(1), 799–818.

Taşkın Z C, Smith J C, Romeijn H E & Dempsey J F 2010 'Optimal Multileaf Collimator Leaf Sequencing in IMRT Treatment Planning' *Operations Research* **58**(3), 674–690.

Tuncel A T, Preciado F, Rardin R L, Langer M & Richard J P P 2012 'Strong Valid Inequalities for Fluence Map Optimization Problem under Dose-Volume Restrictions' *Annals of Operations Research* **196**(1), 819–840.

Wake G M, Boland N & Jennings L S 2009 'Mixed Integer Programming Approaches to Exact Minimization of Total Treatment Time in Cancer Radiotherapy using Multileaf Collimators' *Computers & Operations Research* **36**(3), 795–810.

Wang X, Zhang X, Dong L, Liu H, Wu Q & Mohan R 2004 'Development of Methods for Beam Angle Optimization for IMRT using an Accelerated Exhaustive Search Strategy' *International Journal of Radiation Oncology, Biology and Physics* **60**(4), 1325–1337.

Webb S 2012 'A 4-Bank Multileaf Collimator Provides a Decomposition Advantage for Delivering Intensity-Modulated Beams by Step-and-Shoot' *Physica Medica* **28**(1), 1–6.

Winston W L, Venkataramanan M & Goldberg J B 2003 *Introduction to mathematical programming* Vol. 1 Thomson/Brooks/Cole.

Wolsey L 1998 *Integer Programming* Wiley Series in Discrete Mathematics and Optimization Wiley New York.

Wu X, Dou X, Bayouth J E & Buatti J M 2013 'An Almost Linear Time Algorithm for Field Splitting in Radiation Therapy' *Computational Geometry: Theory and Applications* **46**(6), 673–687.

Zhang Y & Merritt M 2006 *in* 'Multiscale optimization methods and applications' pp. 205–227.